Physico-chemical Properties of Iron-oxide-dextrin Thin Films

CARMEN STELUTA CIOBANU[1,2]*, ECATERINA ANDRONESCU[1], LIVIA PALL[1,3], SIMONA LILIANA ICONARU[2], ENIKÖ GYORGY[3,4], DANIELA PREDOI[2*]

[1]University Politehnica of Bucharest, Faculty of Applied Chemistry and Materials Science, Department of Science and Engineering of Oxide Materials and Nanomaterials, 1 – 7 Polizu Str., 011061, Bucharest , Romania

[2,*]National Institute of Materials Physics, 077125, Magurele, Romania

[3] National Institute for Lasers, Plasma and Radiation Physics, 077125 Bucharest-Magurele, Romania

[4] Instituto de Ciencia de Materiales de Barcelona and Centre d'Investigacions en Nanocičncia i Nanotecnologia, Consejo Superior de Investigaciones Cientificas, Campus UAB, 08193, Bellaterra, Spain

Iron oxide nanoparticles were synthesized in the presence of dextrin. The adsorption process of different dextrin molecules onto the surface of in water dispersed iron-oxide nanoparticles has been investigated to optimize the preparation of iron oxide magnetic fluids. An average iron oxide core size of 8 nm was found by transmission electron microscopy (TEM) for the samples. Scanning electron microscopy (SEM) micro-structural studies revealed a spherical shape of the particles. X-ray phase analysis revealed spinel structure of the iron oxide particles. The attachment of the dextrin on the particle surface was investigated by FTIR spectrometry. The dextrin coated iron oxide nanoparticles were used as targets in Pulsed Laser Deposition (PLD) experiments for thin films synthesis.

Keywords: iron-oxide, dextrin, nanoparticles, thin films

The iron oxide has found numerous applications due to its extraordinary magnetic properties [1]. The magnetic nano-sized particles exhibit the property of super-paramagnetism. The very small crystal size and surface effects have a great influence on the magnetic behaviour of these materials. The iron oxide nanoparticles are also used in important biomedical applications [2-7]. The use of superparamagnetic nanoparticles iron oxide based colloids the contrast agent in magnetic resonance is now a well established area of pharmaceutical development [8-10]. The main problem encountered by all particles used in vivo, however, is adsorption of biological elements, especially proteins [11-17].

In the present investigation we studied the synthesis and properties of bio-compatible magnetic nanoparticles for magnetic resonance imaging. That means that the adsorption process of dextrin occurred during the formation of the iron-oxide nanoparticles. The samples were investigated by Fourier Transform infrared (FT-IR) Spectroscopy, X-ray Diffraction (XRD) Analysis, Scanning Electron Microscopy (SEM), Transmission Electron Microscopy (TEM), X-ray Photoelectron Spectroscopy (XPS), Differential Thermal Analysis (DTA) and Thermal Gravimetric Analysis (TGA).

In this work, we report the synthesis and physico-chemical properties of uncoated and dextrincoated iron-oxide nanoparticles by coprecipitation and pulsed laser deposition (PLD).

Experimental part

Materials and methods

Ferrous chloride tetrahydratate ($FeCl_2 . 4H_2O$), ferric chloride hexahydratate ($FeCl_3 . 6H_2O$), natriun hydratate (NaOH) and dextrin $(C_6H_{10}O_5)_n$ where purchased from Merck. These reagents were used directly as received. De-ionized water was used in the synthesis of nanoparticles, and in the rinsing of clusters.

Synthesis of iron oxide nanoparticles

Iron oxide nanoparticles were prepared according to the following procedure: ferrous chloride tetrahydrate ($FeCl_2 . 4H_2O$) in 2M HCl and ferric chloride hexahydratate ($FeCl_3 . 6H_2O$) were mixed at room temperature (Fe^{2+}/Fe^{3+} = 1/2) [18-21]. The mixture was dropped into 200 mL of 1.5M NaOH solution and vigorous stirred for about 30 min. The resulting precipitate was insolated and the supernatant was removed from the precipitate by decantation. Purified de-ionized water was added to the precipitate and the solution decanted after centrifugation at 8000 rot/min. The product was separated by centrifugation and dried at 40 ^{0}C (sample 1).

Synthesis of dextrin coated iron oxide nanoparticles

Dextrin solution (8.5 g in 85 mL of water) was heated at 90 ^{0}C for 1h with continuous agitation (200 rot/min). Then 40 mL of 5M NaOH was added to the solution. Ferrite solution (30 mL) containing stoichiometric ratio of 1:2 ferrous chloride tetrahydrate ($FeCl_2 . 4H_2O$) and ferric chloride hexahydratate ($FeCl_3 . 6H_2O$) was added dropwise to the solution [22-26]. The suspension was incubated for 1h at 90^{0}C for 1h with gentle stirring. The 5M NaOH was added dropwise to obtain a *p*H of 11 [23-28]. The precipitate were centrifuged and washed with de-ionized water. The product was separated by centrifugation and dried at 40^{0}C (sample 2).

Growth of iron oxide dextrin thin film

The thin film deposition experiments were conducted inside a stainless steel reaction chamber. A frequency quadrupled Nd:YAG laser source (λ = 266 nm, $\tau_{FWHM} \cong 5$ ns, ν=10 Hz) was used for the irradiations. Prior to every deposition the reaction chamber was evacuated with the aid of a high vacuum installation down to a residual pressure of 10^{-4} Pa. The laser beam incidence angle onto the target was chosen of about 45^o. The incident laser fluence was set at values in the range of (0.5-2) J/cm^2. For

& email: dpredoi@infim.ro, dpredoi68@gmail.com; Tel.: 0723751972

Table 1
SAMPLE IDENTIFICATION AS A FUNCTION OF INCIDENT LASER FLUENCE

Sample	Laser fluence [J/cm^2]
DF01	1.5
DF02	0.5
DF03	2
DF04	1

the deposition of each film we applied 12000 subsequent laser pulses. In table 1 is presented the sample identification as a function of incident laser fluence.

The targets were prepared by conventional pressing at 3 MPa of base dextrin coated iron oxide nano-powder material. The Si (100) substrates were placed parallel to the target at a separation distance of 4 cm and maintained at room temperature during the deposition process.

To avoid piercing the targets were rotated during the multipulse laser irradiation with a frequency of 0.4 Hz. The target cleaning was performed with the application of 1000 preliminary laser pulses. During this process a shutter was interposed at the mid-distance between the target and the substrate, parallel to them. Previous experience demonstrated that this proves essential for the elimination of contaminants and impurities present on the target surface.

Sample characterization

The samples were characterized by X-ray diffraction (XRD) with a Philips PW1050 X- ray powder diffractometer using CuK_α incident radiation. An estimation of crystallite sizes was done from the width of the diffraction using the Scherer formula.

Transmission electron microscopy (TEM) studies were carried out using a JEOL 200 CX. The specimen for TEM imaging was prepared from the particles suspension in de-ionized water. A drop of well-dispersed supernatant was placed on a carbon – coated 200 mesh copper grid, followed by drying the sample at ambient conditions before it is attached to the sample holder on the microscope.

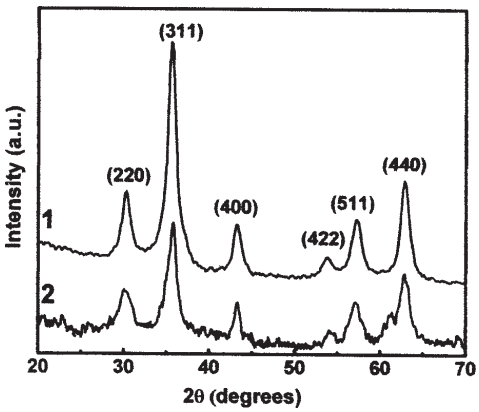

Fig. 1. The X-ray diffraction patterns of sample prepared: (1) iron oxide and (2) iron oxide coated with dextrin

The surface morphology and growth mode of samples were investigated by scanning electron microscopy (SEM) by a XL-30_ESEM TMP device. For the elemental analysis the electron microscope was equipped with an energy dispersive X-ray (EDX) attachment.

IR spectroscopic studies were performed in the range 1800-400 cm^{-1} using FTIR Spectrum BX Spectrometer. Samples dehydrated at room temperature were pelleted with dried KBr.

On the powder, Differential Thermal Analysis and Thermal Gravimetric Analysis were performed using the Shimatzu DTG-TA-50 and DTA 50 analyzer in the 25-800^{0}C temperature range, air environment, and reference made of Al_2O_3.

Results and discussions

The XRD patterns of both uncoated (1) and dextrin coated iron oxide nanoparticles (2) are presented in figure 1. The diffraction lines at 30.2, 35.6, 43.2, 56.2, and 62.8° could be attributed to the (220), (311), (400), (510), and (440) lattice plane reflections of the cubic Fe_3O_4 as well as γ-Fe_2O_3 phases.

The shape and the size distribution of iron oxide and dextrin coated iron oxide nanoparticles were investigated by TEM. As can be seen both the iron oxide (fig. 2) and dextrin coated (fig. 3) nanoparticles are nearly spherical with an average diameter of about 7.0 ±1 nm.

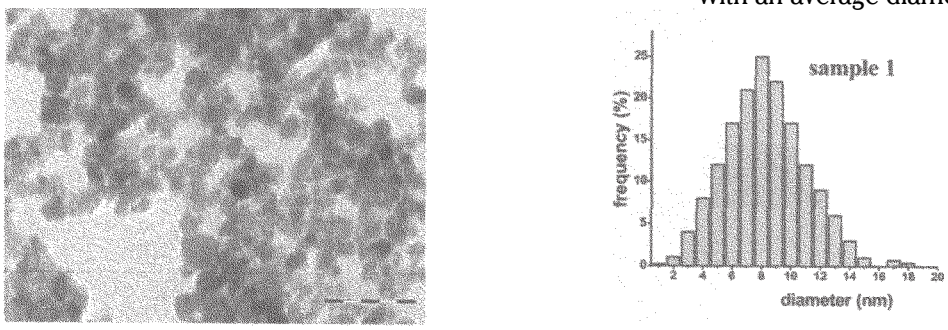

Fig. 2. Transmission electron microscopy images of iron oxide nanoparticles (left) and grain size distribution from TEM of iron oxide (right)

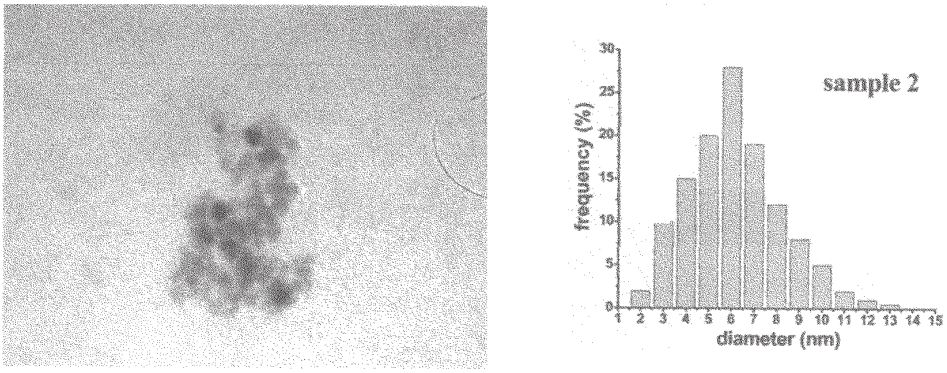

Fig. 3. TEM images of iron oxide nanoparticles coated dextrin (left) and grain size distribution from TEM of iron oxide nanoparticles coated with dextrin (right)

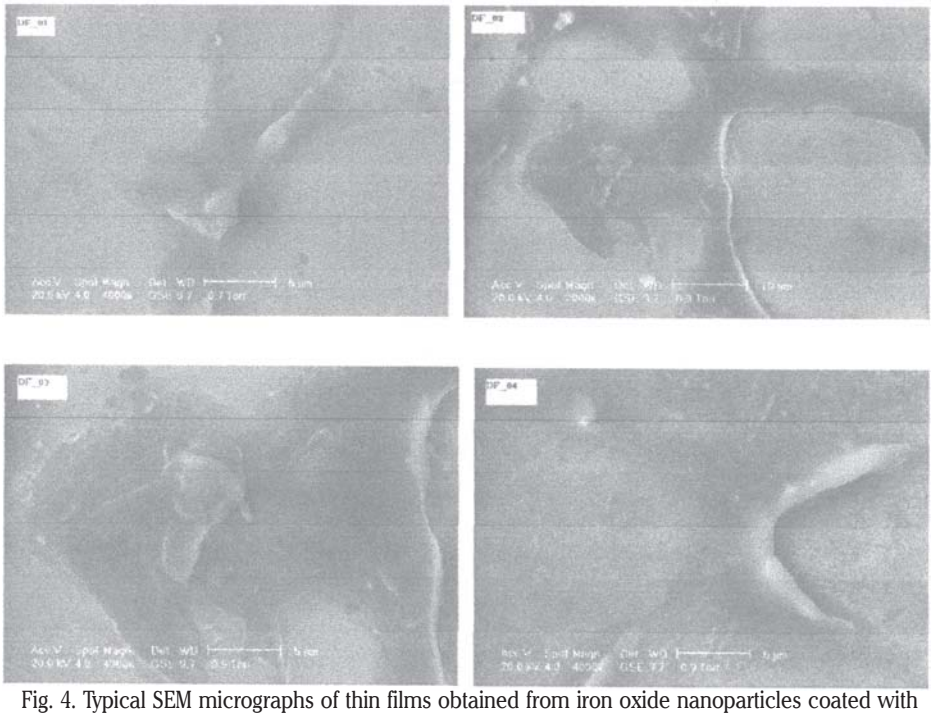

Fig. 4. Typical SEM micrographs of thin films obtained from iron oxide nanoparticles coated with dextrin DF01 (1.5 J/cm^2 laser fluence), DF02 (0.5 J/cm^2 laser fluence), DF03 (2 J/cm^2 laser fluence), DF04 (1 J/cm^2 laser fluence)

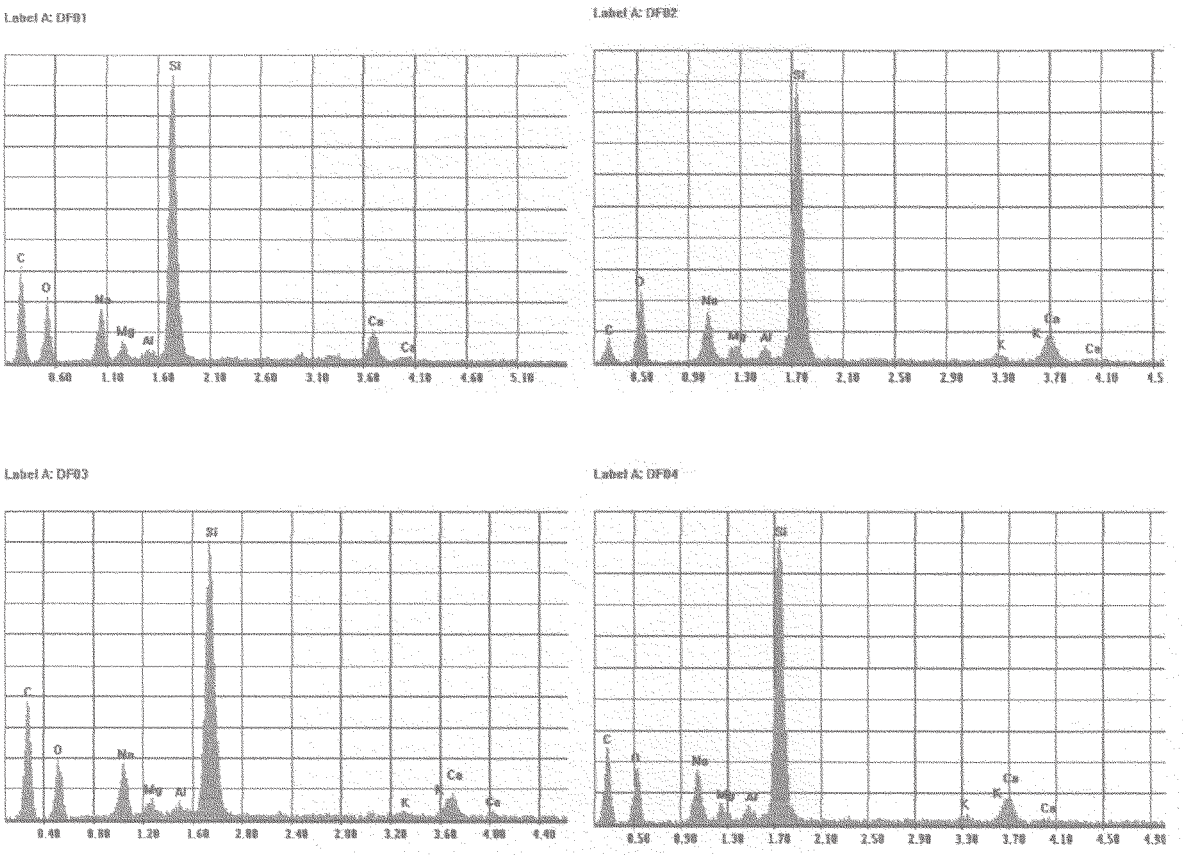

Fig. 5. EDS spectra of thin films obtained from iron oxide nanoparticles coated with dextrin DF01 (1.5 J/cm^2 laser fluence), DF02 (0.5 J/cm^2 laser fluence), DF03 (2 J/cm^2 laser fluence), DF04 (1 J/cm^2 laser fluence)

Results obtained by scanning electron microscopy analysis for the iron oxide-dextrin thin films are shown in figure 4. To analyze the morphology and crystallite size, a SEM analysis has been conducted. Some sphere-shaped protuberances can be observed on the surface of thin films with almost the same aspect for sample DF01 and DF02.

We note that the EDS spectra (fig. 5) can be used in this case only for a qualitative analysis. Indeed, a quantitative analysis is not possible as the oxygen $K\alpha_{1,2}$ lines includes contributions both from the thin films and from SiO_2 substrate. Hydrogen is missing singe as known, elements lighter than boron cannot be detected by EDS.

The attachment of the dextrin on the magnetite particle surface was further confirmed by TGA. The TGA curves of samples 1, 2 and pure dextrin (D) were shown in figure 6. In our samples it was observed that the percentage of

weight loss is more important when the magnetite nanoparticles were coated with dextrin (52.68%) compared to that of iron oxide (3.04%). TGA thermogram of sample 2 show a continuous weight loss in the range of decomposition temperature for dextrin (compare parts D and 2 of the fig. 6).

The attachment of the dextrin on the iron oxide nanoparticles surface was further confirmed by TGA. TGA results show three-step weight loss for iron oxide nanoparticles coated with dextrin (fig. 7). The weight loss is 91.9%. The first weight loss stage occurs from 30 to 270 ^{0}C. This weight loss is due to the evaporation of absorbed water from the surface. At the second stage, a rapid weight loss can be observed from 270 to 340 ^{0}C in agreement with the transformation of Fe_3O_4 to γ- Fe_2O_3 occurring around 300 ^{0}C [18-20, 29]. The percentage of weight loss in this temperature range is about 69.71%. It can, however, be seen that the weight of sample continuously, decreased with increasing temperature from 340 to 800 ^{0}C. This may be due to the combustion of organic residues and of subsequent carbon composition.

The attachment of the dextrin on the iron oxide particles surface was investigated by FT-IR spectroscopy. Figure 8 gives the FT-IR transmission spectra of iron oxide (a), and pure dextrin (b) and iron oxide nanoparticles coated with dextrin (c). In figure 9 can be observed that the films studied have a similar behaviour.

The assignments of the absorption band in the spectra are listed in table 2. The spectrum corresponding to iron oxide nanoparticles contain characteristic OH stretching,

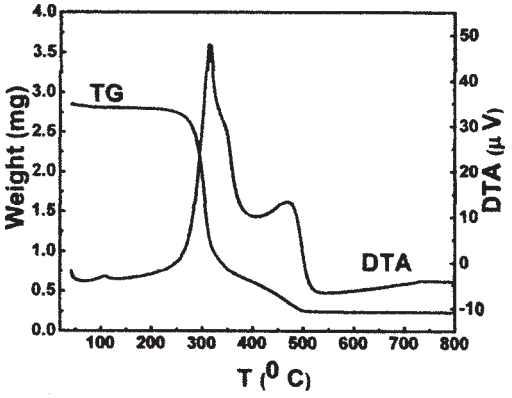

Fig. 7. TGA for iron-oxide-dextrin nanoparticles powder (trace at a heating rate of 10 ^{o}C / min in air)

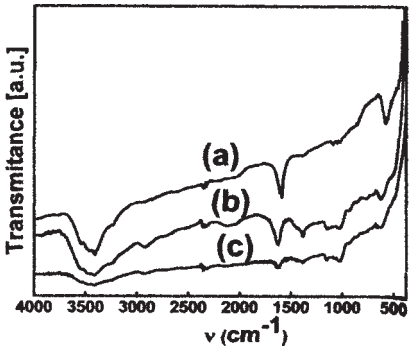

Fig. 8. The FT-IR spectra of samples: (a) iron oxide, (b) pure dextrin and (c) iron oxide nanoparticles coated with dextrin

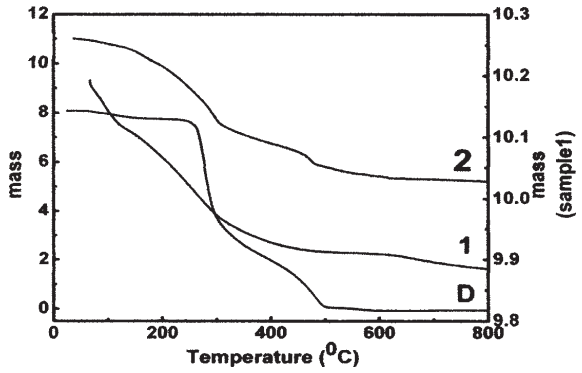

Fig. 6. THE TGA curves of sample 1,2 and pure dextrin

ν O-H, vibration bands at 1600 cm^{-1} the most probably due to the adsorbed water molecules [18-19]. This band is missing from the spectra of dextrin coated iron oxide nanoparticles and thin films. This can be attributed to the additional incubation step at 90 °C for 1 h included in the synthesis process. The band observed between 620 cm^{-1} and 580 cm^{-1} in the spectra of iron oxide nanoparticles and dextrin coated nanoparticles and thin films corresponds to the ν Fe-O stretching vibration [22, 25].

The FT-IR spectrum of pure dextrin powder contains a band between 1040-1110 cm^{-1} corresponding to the ν C-

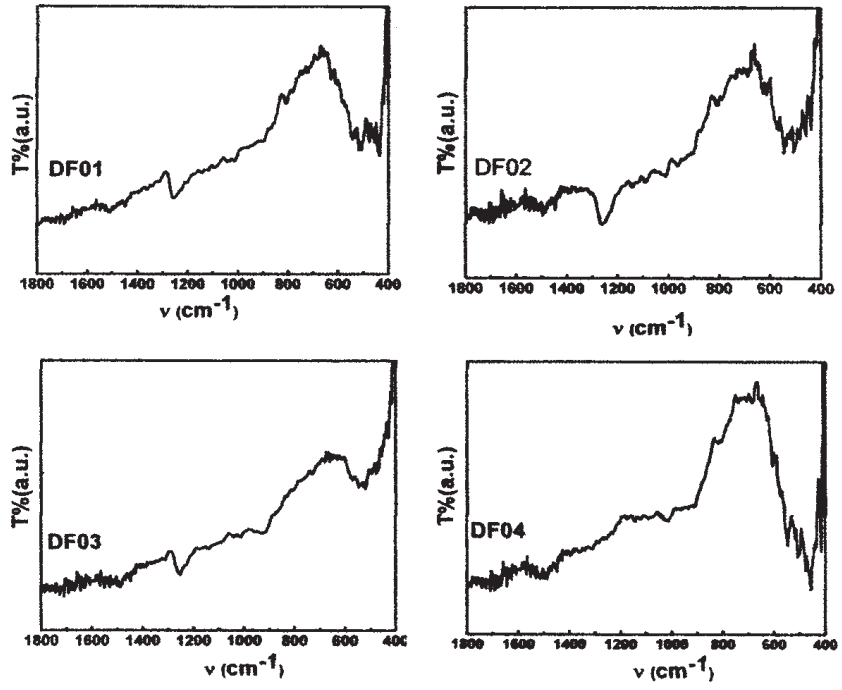

Fig. 9. IR spectra of thin films obtained from iron oxide nanoparticles coated with dextrin DF01 (1.5 J/cm^2 laser fluence), DF02 (0.5 J/cm^2 laser fluence), DF03 (2 J/cm^2 laser fluence), DF04 1 J/cm^2 laser fluence)

Dextrin	Iron oxide nanoparticles coated with dextrin (cm^{-1})	Iron-oxide nanoparticles (cm^{-1})	Assignments
3500-3200	3500	3500	ν^* H- O……H
2925	2917		ν^*_{as} C-H of $-CH_2$
1455; 1370	1460; 1350	1600	δ^*H-C-OH
1277	1273		δ^*H-C-OH
1152	1160		ν^*_s C-O-C
800-1200	800-1200		C-C
	590	590	Fe-O

Table 2
ASSIGNMENT OF THE ABSORPTION BANDS IN THE IR SPECTRA

Notations used: ν^*: stretching vibration; ν^*_{as}: asymmetrical stretching vibration; ν^*_s: symmetrical stretching vibration; δ^*: deformation

O-C stretching vibration, a band around 900 cm^{-1} which could be associated with the ν C-C stretching vibration, as well as at 1400 cm^{-1} of the δ H-C-OH vibration [22, 25-26].The band at 1600 cm^{-1} correspond to adsorbed water molecules is also present in the spectra of pure dextrin powder.

Besides the band corresponding to the ν Fe-O stretching vibration between 620 and 580 cm^{-1} the spectra of dextrin coated iron oxide nanoparticles and thin films contains a band at around 900 cm^{-1} corresponding to the νC-C stretching vibration [30-31]. In addition, the spectra of the thin film present a band at around 1300 cm^{-1} which could be attributed to the δ H-C-OH vibration.

Conclusions

Iron oxide nanoparticles coated with the dextrin were synthesized by coprecipitation of two mains solutions $FeCl_2 . 4H_2O$ and $FeCl_3 . 6H_2O$ in a stoichiometric ratio 1:2 in dextrin solution adding 5M NaOH. The iron oxide phase was described to be a ferrite with properties of magnetite. The TEM images suggest that the use of dextrin in the material synthesis limits particle size. The iron oxide-dextrin preparation generates particles that are significantly smaller than the iron oxide preparation in which dextrin is not present. Moreover the adsorption dextrin iron oxide nanoparticles were evidenced by FTIR spectroscopy and were confirmed by TG analysis.

Acknowledgements: This work was financially supported by the Romanian Ministry for Education and Research under the contracts PNCDI-II 71-097/2007 and POSDRU ID 7713) and the Spanish Ministry of Education and Science under the contract MAT2006-26534-E.

References

1. VELASCO-GARCIA MN., MOTTRAM T. Biosyst. Eng. ,**84**, No. 1, 2003.
2. FU L., DRAVID V.P., JOHNSON D.L. Appl. Surf. Sci. **181**, No. 173, 2001
3. ALEXIAON C., ARNOLD W., HULIN P., KLEIN R.J., RENZ H., PARAK F.G., BERGEMANN C., LÜBBE A.S., J. Magn. Magn. Mater, **225,** No. 187, 2001
4. JORDAN A., ACHOLZ R., WUST P., FÄHLING H., FELIX R. J. Magn. Magn. Mater, **201**, No. 413, 1999
5. ATKINSON I., TEOREANU I., ZAHARESCU M., Rev. Chim. (Bucharest), **59**, no. 9, 2008, p. 990
6. JIPA S., GHEORGHIU L.M., Rev. Chim. (Bucharest), **56**, no. 3, 2005, p. 254
7. ZAHARESCU M., RAILEANU M., MIHAIU S., Rev. Chim. (Bucharest), **43**, No. 9, 1992, p. 557
8. RUNGE V.M., RIJCEN T.H., DAVIDOFF A., WELLS J.W., STARK D.D. J. Magn. Reson. Imaging **4**, 1994, p. 281-289.
9. PORTET D., DENOIT B., RUMP E., LEJEUNNE J.J., JALLET P. J. Colloids interface Sci. , **238**, 2001, p. 37
10. RAMGE P., UNGER R.E., OLTROGGE J.B., ZENKER D., BEGLLY D., KREUER J., BRIESEN H. VON. Eur. J. Neurol., **12**, 2000, p. 1931-1934.
11. ANDRONESCU, E., NICOLA, O., BIRSAN, C., GHITULICĂ, C., Romanian Journal of Materials, **3**, no.72, 2007, p. 122
12. NICOLA, O., ANDRONESCU, E., GHITULICĂ, C., PALL L., Romanian Journal of Materials, **36,** No.4**,** 2006, p. 261
13.. LUNGU, A., ALBU, M.G., TRANDAFIR, V., Mat. Plast., **44**,no. 4, 2007, p.273
14. FICAI, A., ANDRONESCU, E., GHITULICĂ, C., VOICU, G., TRANDAFIR, V., MÂNZU, D., FICAI, M., PALL, S.T.., Mat. Plast., **46**, no. 1 , 2009, p.11
15. ZAHARESCU M., RUSSU R., RAILEANU M., Rev. Chim. (Bucharest), **47**, no. 6, 1996, p. 941
16. RAILEANU M., Revue Roum. Chim., **51**, No.10, 2006, p. 533
17. ZAHARESCU M., RAILEANU M., MIHAIU S., Rev. Chim. (Bucharest), **42**, no. 8-9, 1991, p.406
18. PREDOI D., CHANEAC C., TRONC E., JOLIVET J.P., CHERKAOUR R., EZZIR A., NOGUES M., DORMANN J.L. Journal of Magnetism and Magnetic Materials. **203**, 1999, p. 63
19. PREDOI D., VATASESCU-BALCAN R.A. Journal of Optoelectronics and Advanced Materials., **10,** No. 1**,** 2008, p. 152
20. PREDOI D., BARSAN M., ANDRONESCU E., VATASESCU-BALCAN R.A., COSTACHE M. Journal of Optoelectronics and Advanced Materials.; **9,** No.11**,** 2007, p. 3609-3613.
21.BERRY C.C., WELLS S., CHARLES S., AITCHISON G., CURTIS A.S.G. Biomaterials., **25**, 2004, p. 5405
22. PREDOI D., VALSANGIACOM C.M., Journal of Optoelectronics and Advanced Materials, **9,** No**.** 6, 2007, p. 1797
23. VATASESCU-BALCAN R.A., PREDOI D., UNGUREANU F., COSTACHE M., Journal of Optoelectronics and Advanced Materials **10**, No. 3, 2008, p. 693
24. PREDOI D., CRISAN O., JITIANU A., VALSANGIACOM M.C., RAILEANU M., CRISAN M., ZAHARESCU M., Thin Solid Films **16**, 2007,p.6319
25. PREDOI D., Digest Journal of Nanomaterials and Biostructures **2**, 2007, p.169
26. VATASESCU-BALCAN, R.A.; PREDOI, D., COSTACHE, M., Febs Journal , 275, 2008, p. 374
27.Rollet AP, Bouaziz R. GAUTHIER-VILLARS, EDITEUR, 55 quai des Grands-Augustins, Paris 6e
28. HAIR ML. J. Non-Cryst. Solids. **19,** 1975, p. 299
29. BARRODO E, PRIETO F, MEDINA J, LOPEZ FA. J. Alloys. Compd. **335**, No. 203, 2002
30. MARTIN DE VIDALES JL, LOPEZ-DELGADO A, VILA E, LOPEZ FA. J. Alloys. Compd. **287,** No**.** 276, 1999
31.WANG HR, CHEN KM. Colloids and Surfaces A. Physicochem. Eng.Aspects, **281**, No. 190, 2006

Manuscript received: 25.09.2010